nature genetics

Exome sequencing identifies *BRAF* mutations in papillary craniopharyngiomas

Priscilla K Brastianos[1–5,22], Amaro Taylor-Weiner[5,22], Peter E Manley[6,22], Robert T Jones[4,7], Dora Dias-Santagata[3,8], Aaron R Thorner[4,7], Michael S Lawrence[5], Fausto J Rodriguez[9], Lindsay A Bernardo[8], Laura Schubert[7], Ashwini Sunkavalli[7], Nick Shillingford[10], Monica L Calicchio[10], Hart G W Lidov[3,10,11], Hala Taha[12], Maria Martinez-Lage[13], Mariarita Santi[14], Phillip B Storm[15,16], John Y K Lee[15], James N Palmer[15,17], Nithin D Adappa[17], R Michael Scott[3,18], Ian F Dunn[3,19], Edward R Laws Jr[3,19], Chip Stewart[5], Keith L Ligon[3,4,10,11], Mai P Hoang[3,8], Paul Van Hummelen[4,7], William C Hahn[3–5,7], David N Louis[3,8], Adam C Resnick[15,16], Mark W Kieran[3,6,20,23], Gad Getz[3,5,8,23] & Sandro Santagata[3,10,11,21,23]

Craniopharyngiomas are epithelial tumors that typically arise in the suprasellar region of the brain[1]. Patients experience substantial clinical sequelae from both extension of the tumors and therapeutic interventions that damage the optic chiasm, the pituitary stalk and the hypothalamic area[2–4]. Using whole-exome sequencing, we identified mutations in *CTNNB1* (β-catenin) in nearly all adamantinomatous craniopharyngiomas examined (11/12, 92%) and recurrent mutations in *BRAF* (resulting in p.Val600Glu) in all papillary craniopharyngiomas (3/3, 100%). Targeted genotyping revealed BRAF p.Val600Glu in 95% of papillary craniopharyngiomas (36 of 39 tumors) and mutation of *CTNNB1* in 96% of adamantinomatous craniopharyngiomas (51 of 53 tumors). The *CTNNB1* and *BRAF* mutations were clonal in each tumor subtype, and we detected no other recurrent mutations or genomic aberrations in either subtype. Adamantinomatous and papillary craniopharyngiomas harbor mutations that are mutually exclusive and clonal. These findings have important implications for the diagnosis and treatment of these neoplasms.

Craniopharyngiomas occur at an average age-adjusted incidence rate of 0.18 per 100,000 (ref. 5). There are two main subtypes of craniopharyngiomas—the adamantinomatous form that is more common in children and the papillary form that occurs predominantly in adults. Located in or above the sella turcica, craniopharyngiomas grow adjacent to the optic chiasm and often extend to involve the hypothalamus, cranial nerves, ventricular system, visual pathways and major blood vessels at the base of the brain. Curative surgery is exceedingly difficult[6], and resection can contribute to complications. The spectrum of complications include visual defects, severe headaches, pan-hypopituitarism, impaired intellectual function and wide-ranging hypothalamic dysfunction leading to sleep disorders[7], abnormal thermoregulation and diabetes insipidus, as well as to hyperphagia and uncontrollable obesity[2–4]. Aptly, Harvey Cushing, the father of neurosurgery, who introduced the term 'craniopharyngioma' declared them "the most formidable of intracranial tumors."[8,9]

Knowledge of the molecular mechanisms that drive craniopharyngiomas remains limited, which has hampered the development of systemic therapies for this type of tumor. Mutations in exon 3 of *CTNNB1* (β-catenin), which encodes a degradation targeting motif, have been described in adamantinomatous craniopharyngiomas, occurring in 60–75% of patients in most published series[10–12]. However, mutations that drive the growth of papillary craniopharyngiomas have not been identified. To that end, we performed massively

[1]Division of Hematology/Oncology, Massachusetts General Hospital, Boston, Massachusetts, USA. [2]Division of Neuro-Oncology, Massachusetts General Hospital, Boston, Massachusetts, USA. [3]Harvard Medical School, Boston, Massachusetts, USA. [4]Department of Medical Oncology, Dana-Farber Cancer Institute, Boston, Massachusetts, USA. [5]Broad Institute of MIT and Harvard, Boston, Massachusetts, USA. [6]Department of Pediatric Oncology, Dana-Farber Cancer Institute, Boston, Massachusetts, USA. [7]Center for Cancer Genome Discovery, Dana-Farber Cancer Institute, Boston, Massachusetts, USA. [8]Department of Pathology, Massachusetts General Hospital, Boston, Massachusetts, USA. [9]Department of Pathology, Johns Hopkins University, Baltimore, Maryland, USA. [10]Department of Pathology, Boston Children's Hospital, Boston, Massachusetts, USA. [11]Department of Pathology, Brigham and Women's Hospital, Boston, Massachusetts, USA. [12]Children's Cancer Hospital Egypt, Cairo, Egypt. [13]Department of Pathology and Laboratory Medicine, Hospital of the University of Pennsylvania, Philadelphia, Pennsylvania, USA. [14]Department of Pathology, Children's Hospital of Philadelphia, Philadelphia, Pennsylvania, USA. [15]Department of Neurosurgery, Hospital of the University of Pennsylvania, Philadelphia, Pennsylvania, USA. [16]Division of Neurosurgery, Children's Hospital of Philadelphia, Philadelphia, Pennsylvania, USA. [17]Department of Otorhinolaryngology–Head and Neck Surgery, Hospital of the University of Pennsylvania, Philadelphia, Pennsylvania, USA. [18]Department of Neurosurgery, Boston Children's Hospital, Boston, Massachusetts, USA. [19]Department of Neurosurgery, Brigham and Women's Hospital, Boston, Massachusetts, USA. [20]Department of Pediatrics, Boston Children's Hospital, Boston, Massachusetts, USA. [21]Department of Cancer Biology, Dana-Farber Cancer Institute, Boston, Massachusetts, USA. [22]These authors contributed equally to this work. [23]These authors jointly directed this work. Correspondence should be addressed to P.K.B. (pbrast@broadinstitute.org), G.G. (gadgetz@broadinstitute.org) or S.S. (ssantagata@partners.org).

Received 3 November 2013; accepted 9 December 2013; published online 12 January 2014; doi:10.1038/ng.2868

parallel sequencing of 15 craniopharyngiomas from both subtypes and targeted genotyping in samples from 95 additional patients.

We first used whole-exome sequencing to analyze the DNA from a discovery cohort of adamantinomatous (n = 12) and papillary (n = 3) craniopharyngiomas (**Supplementary Table 1**). As craniopharyngiomas are often heterogeneous tumors with nests of tumor cells interspersed between large amounts of reactive tissue and stromal cells, we expected the mutations to have low allelic fractions (i.e., the mutations might only be found in a small subset of the sequenced cells because of substantial contamination by normal cells). Thus, we analyzed the sequencing data with a recently described method—MuTect—that uses a Bayesian classifier to identify somatic mutations with very low allelic fractions coupled with filters that provide high specificity[13].

In consonance with the benign histology of these tumors, we identified only a relatively small number of nonsynonymous somatic mutations in both craniopharyngioma subtypes when compared to large cohorts of other tumor types[14] (**Fig. 1**). The nonsynonymous mutation rate of 0.9 per Mb in the craniopharyngioma samples was similar to that found in a number of pediatric tumors, as well as that in low-grade tumors in adults, for example, World Health Organization–classified grade I meningioma[15] (**Fig. 1**). 58% of the mutations were cytosine to thymidine at CpG dinucleotides, which is consistent with spontaneous deamination and not a carcinogen-induced process (**Fig. 1**)[14]. As we anticipated, the allelic fraction for many of the mutations was very low (median, 3%; range, 0.96–48%).

The most frequently mutated gene was *CTNNB1*, with mutations in this gene present in 11 of 12 adamantinomatous craniopharyngiomas (**Fig. 2** and **Supplementary Tables 2–4**). These events overlapped with mutations previously described in this tumor type and were located in exon 3 exclusively[10,12]. In addition, adamantinomatous craniopharyngiomas harbored isolated mutations in genes that have been implicated previously in cancer (**Fig. 2**). We identified mutations in genes listed in the Cancer Gene Census[16] that are involved in transcriptional regulation (*BCOR*, *CRTC3*, *MITF* and *PRDM1*) and epigenetic regulation (*KDM5A* and *SMARCA4*), as well as in DNA repair (*BRCA2*) (**Fig. 2**). We detected additional mutations in genes not listed in the Cancer Gene Census but that have described roles in cancer, including genes involved in chromatin remodeling and regulation of transcription (including *ASCC2*, *KAT5*, *PIWIL1*, *SIN3A* and *SMC1A*), cell cycle and DNA repair (including *ATR*, *BARD1*, *CDC25B*, *HBP1*, *RBBP8* and *RTEL1*) and cell adhesion (*ITGA3*, *PKD1*, *PKD1L1*, *PODN*, *ROCK1* and *RPTN*)[16]. However, many of these may be passenger mutations that do not contribute to tumor initiation or progression.

All three of the papillary craniopharyngiomas in our discovery set harbored mutations (c.1799T > A) in the well-established oncogene *BRAF* (resulting in p.Val600Glu) that have been shown to constitutively activate this serine-threonine kinase that regulates MAP kinase (also called ERK) signaling and affects cell division and differentiation (**Fig. 2**). None of the three papillary craniopharyngiomas had mutations in *CTNNB1*. Although two of these samples were resected from adults (31 and 52 years old), one of the samples was from a rare papillary craniopharyngioma that occurred in a child (9 years old), suggesting a similar pathogenesis between pediatric and adult papillary craniopharyngiomas. We did not identify mutations in other genes listed in the Cancer Gene Census in these tumors, but we did note isolated mutations in other genes with potential roles

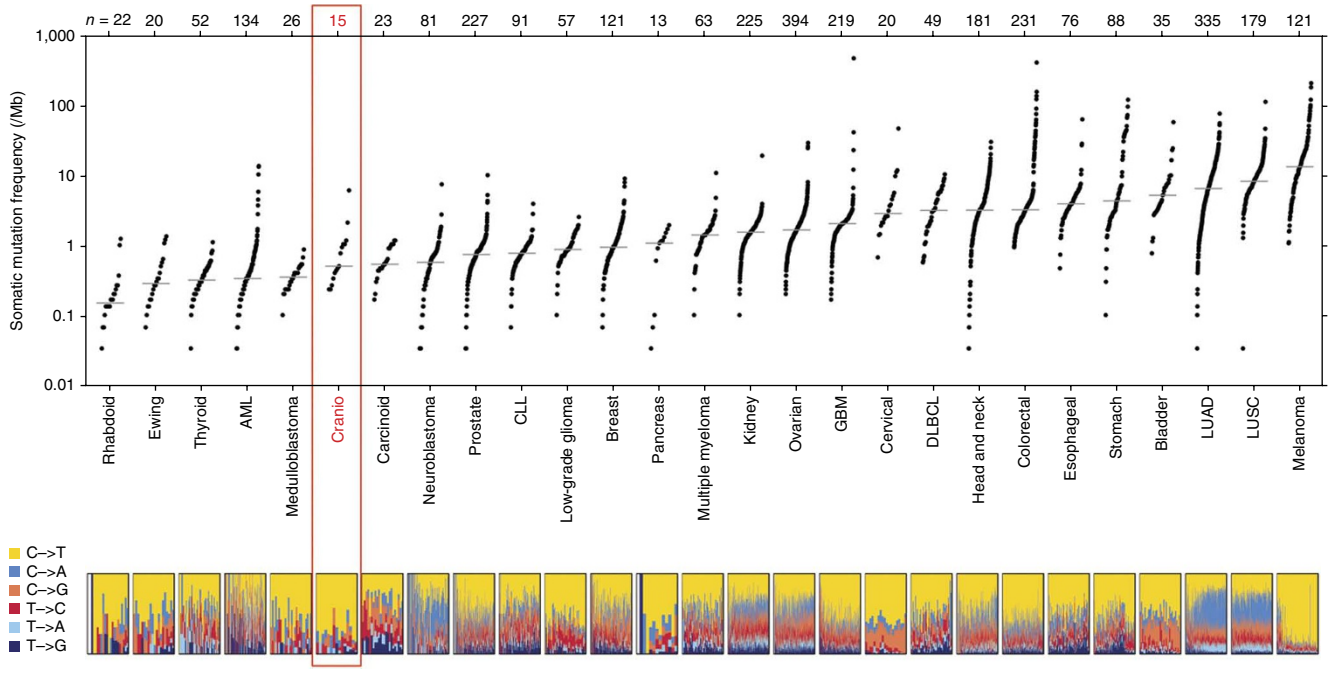

Figure 1 Plot of the number of nonsynonymous mutations per megabase in craniopharyngiomas (n = 15) in comparison to a broad range of pediatric and adult tumors (n = 3,083). Data for all other tumor types, as well as the figure design, were taken from Lawrence *et al.*[14]. Each dot in this plot corresponds to a matched tumor-normal pair. The vertical position indicates the frequency of somatic mutations in that exome. Tumor types are ordered on the basis of their median nonsynonymous frequency, and within each tumor type, tumor-normal pairs are ordered from lowest to highest frequency. The relative proportions of six different possible base-pair substitutions are indicated at the bottom. Craniopharyngioma data are derived from whole-exome sequencing of 15 tumor-normal pairs, including 12 adamantinomatous and 3 papillary craniopharyngioma, and are marked in red. AML, acute myelogenous leukemia; CLL, chronic lymphocytic leukemia; cranio, craniopharyngioma; DLBCL, diffuse large B-cell lymphoma; GBM, glioblastoma multiforme; LUAD, lung adenocarcinoma; LUSC, lung squamous cell carcinoma.

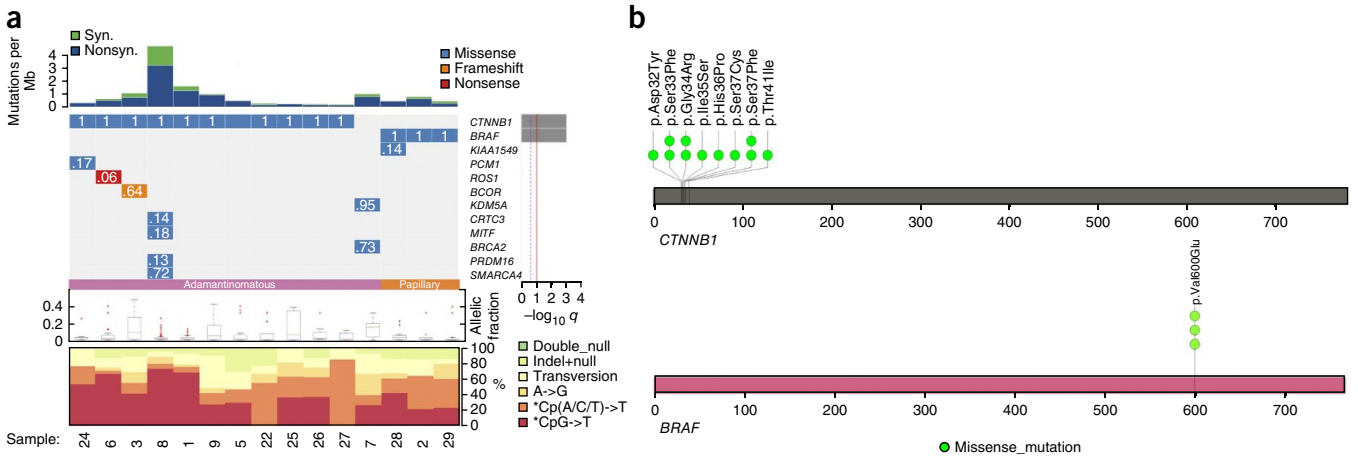

Figure 2 Mutations in adamantinomatous and papillary craniopharyngiomas. (**a**) The number of mutations per megabase in each of 15 craniopharyngioma whole-exome sequencing data sets (12 adamantinomatous and 3 papillary samples). Specific genes are shown that bear nonsynonymous somatic mutations in genes listed in the Cancer Gene Census[16]. Right, false discovery rate *q* values providing the significance of the mutations in each listed gene. Cancer-relevant genes that are not listed in the Cancer Gene Census are not shown. The *q* value is an evaluation of whether a gene is significantly mutated above the expected basal rate of mutation. The *q* values for *BRAF* and *CTNNB1* are both <0.00001. The *q* values of the other genes in the plot are equal to 1. A full list of mutated genes is provided in **Supplementary Table 2**. Colors indicate the type of genetic change identified. Only one mutation is indicated, even if multiple mutations were found in a particular gene. The CCF (0–1.0) for each indicated mutation is shown in white in the corresponding box. The allelic fraction for mutations in each sample is shown in the box plot, with the median indicated by a red line (the allelic fraction for each mutation is listed in **Supplementary Table 2**). The bottom and the top of the boxes represent the first and third quartiles, respectively; the ends of the whiskers represent 1 s.d. above and below the median of the data; and the red dots represent outlier points not included in the whiskers. For each sample, the relative frequencies of six different possible base-pair substitutions are shown at the bottom. Syn., synonymous; nonsyn., nonsynonymous. (**b**) Schematics for *CTNNB1* and *BRAF* indicating the location of the identified mutations (11 in *CTNNB1* and 3 in *BRAF*).

in cancer, including genes encoding chromatin remodeling factors (*CHD5* and *CHD6*)[17] and cell adhesion molecules (*CDH26* and *PTPRT*)[18] and one gene (*KIAA1549*) that is fused to *BRAF* in most cases of pilocytic astrocytoma[19,20]. These mutations, similarly to some of those found in adamantinomatous craniopharyngiomas, may also be passenger mutations.

We used MutSig[14] to analyze the list of mutations identified in our discovery cohort of 15 cases to identify genes that are significantly mutated. Although our cohort is small compared to those from other genomic studies[14] (**Fig. 1**), the prevalence of mutations in *CTNNB1* and *BRAF* was so high that we were readily able to detect these mutations as being statistically significant (**Fig. 2**).

To validate our findings, we used targeted genotyping approaches to analyze an additional 98 craniopharyngioma samples (from 95 different patients) for mutations in the most commonly mutated genes in our discovery cohort—*BRAF* and *CTNNB1*. We also performed immunohistochemistry (IHC) using an antibody (VE1) that selectively recognizes the BRAF p.Val600Glu mutant epitope and not the wild-type epitope from BRAF[21]. In addition, we evaluated the activation status of β-catenin using an antibody that allowed us to detect nuclear (activated) and membranous (inactivated) β-catenin[12]. In total, our validation cohort consisted of 39 papillary craniopharyngioma tumors from 36 different patients and 59 adamantinomatous craniopharyngioma tumors, each from a different patient (**Supplementary Table 1**). Although we detected *CTNNB1* mutations in the adamantinomatous craniopharyngioma samples (51 of 53 samples, 96%), none of these samples harbored *BRAF* mutations (resulting in p.Val600Glu, p.Val600Asp, p.Val600Leu, p.Val600Met or p.Val600Lys). We identified cytoplasmic and nuclear β-catenin by IHC in all of the adamantinomatous samples tested, but β-catenin was localized exclusively to the cytoplasmic membrane in all papillary craniopharyngioma samples tested (**Fig. 3** and **Supplementary Table 1**).

Remarkably, by targeted genotyping and IHC, we detected the p.Val600Glu alteration in 34 of the 36 patients with papillary craniopharyngiomas (94.4%) (**Supplementary Table 1**).

The allelic fraction of mutations (including those in *BRAF* and *CTNNB1*) in our whole-exome data was low (**Fig. 2a** and **Supplementary Table 2**). This raised the possibility of genetic heterogeneity in our tumor samples. To assess this possibility, we used a recently developed computational method (Online Methods) that corrects for tumor purity and estimates the fraction of cancer cell nuclei that harbor a particular mutation (cancer cell fraction; CCF). Although these methods demonstrated that most of the somatic mutations identified in our samples were indeed subclonal, we found that the mutations in *BRAF* and *CTNNB1* were clonal (i.e., they were present in all tumor cells) in the analyzed samples (**Figs. 2a** and **4a** and **Supplementary Table 2**).

To further validate our analysis of intratumor heterogeneity, we reviewed the pattern and distribution of BRAF staining in the

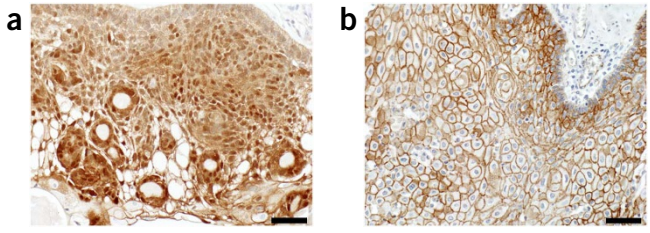

Figure 3 β-catenin localization is different in adamantinomatous and papillary craniopharyngiomas. Shown are IHCs for β-catenin. (**a**) β-catenin is localized to the cytoplasm and the nucleus in an adamantinomatous craniopharyngioma. (**b**) β-catenin is localized to the cell membrane in a papillary craniopharyngioma. Scale bars, 50 μm. β-catenin localization in many samples from the discovery and validation cohort is reported in **Supplementary Table 1**.

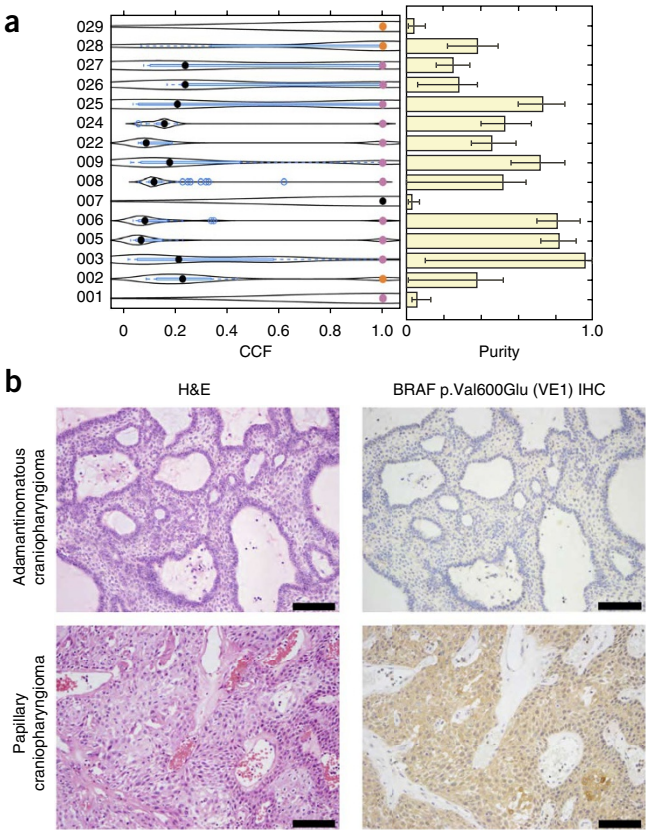

Figure 4 *BRAF* and *CTNNB1* mutations are clonal in craniopharyngiomas. (**a**) Left, a violin plot showing the CCFs for mutations in *BRAF* (orange) and *CTNNB1* (pink) in each tumor analyzed with whole-exome sequencing. The median CCF of all nonsynonymous somatic mutations for each sample is represented by a black dot. Right, bar graph showing the computed purity for each sample (Online Methods); error bars, s.e.m. (**b**) Hematoxylin and eosin (H&E) staining of adamantinomatous and papillary craniopharyngiomas. IHC shows that adamantinomatous craniopharyngiomas are negative for BRAF p.Val600Glu but that there is a diffuse distribution of BRAF p.Val600Glu mutant protein in the neoplastic epithelium of papillary craniopharyngiomas. Stromal elements in the fibrovascular cores of the papillary tumors are negative for the BRAF p.Val600Glu mutant protein. Scale bars, 100 μm.

craniopharyngioma samples (**Supplementary Table 1**). Using the antibody selective for BRAF p.Val600Glu, we did not detect BRAF p.Val600Glu in the adamantinomatous craniopharyngioma samples (**Supplementary Table 1**) or in two of the papillary craniopharyngioma samples with wild-type *BRAF* that we tested (**Fig. 4b**). In the genetically confirmed BRAF p.Val600Glu mutant samples, however, we observed widespread immunoreactivity across the tumor cell population. In these samples, lymphocytes and stromal cells of the fibrovascular core of the tumors were not immunoreactive, but the squamopapillary tumor epithelium stained diffusely for BRAF p.Val600Glu. This observation supports the conclusion that *BRAF* mutations are present uniformly throughout the neoplastic epithelial cells.

Our whole-exome sequencing data of craniopharyngiomas demonstrates that the adamantinomatous and papillary subtypes have distinct molecular underpinnings, each driven principally by mutations in a single well-established oncogene: *CTNNB1* (β-catenin) in the adamantinomatous form and *BRAF* in the papillary form, independent of age.

These mutations appear to be critical events in the pathogenesis of these tumors for several reasons. First, the high prevalence of mutations in *CTNNB1* and *BRAF* in craniopharyngiomas occurs among an overall paucity of additional mutations, supporting that these particular mutations are likely instrumental to the growth of these tumors. Second, the mutations are clonal and segregate perfectly with their respective histologic subtypes, indicating that they are defining genetic aberrations. Moreover, the frequencies of these *CTNNB1* and *BRAF* mutations are much higher in craniopharyngiomas than in most other tumor types that bear these mutations.

Given the mutual exclusivity of mutations in *BRAF* and *CTNNB1*, immunohistochemistry for BRAF p.Val600Glu and β-catenin could be used to routinely distinguish papillary from adamantinomatous craniopharyngiomas and thereby direct patients to appropriate clinical trials. Whereas agents that target WNT signaling remain in development[22,23], the availability of BRAF inhibitors such as vemurafenib[24–29] and dabrafenib[30,31] suggests that patients with papillary craniopharyngiomas could benefit immediately from such targeted therapeutics. These agents have shown a robust clinical response against BRAF p.Val600Glu mutant melanomas[25] and hairy cell leukemias[32], as well as brain tumors such as pleomorphic xanthoastrocytoma[33,34] and ganglioglioma[34,35]. Trials of these therapeutics for papillary craniopharyngiomas should be explored in patients with either residual or recurrent tumors after surgical resection. In addition, BRAF inhibitors could be evaluated as a first-line therapy to be used before surgical resection or radiation therapy.

In summary, our discovery of frequent and clonal mutations in adamantinomatous and papillary craniopharyngioma in *CTNNB1* and *BRAF*, respectively, offers valuable opportunities for testing molecularly guided therapeutics for the treatment of these formidable brain tumors.

URLs. Picard tools, http://picard.sourceforge.net/; SAMtools, http://samtools.sourceforge.net/; Genome Analysis Toolkit (GATK), http://www.broadinstitute.org/gatk; Firehose, https://confluence.broadinstitute.org/display/GDAC/Home; Oncotator, http://www.broadinstitute.org/oncotator.

METHODS

Methods and any associated references are available in the online version of the paper.

Accession codes. Data, including sequence data and analyses, will be available for download from the database of Genotypes and Phenotypes (dbGaP) under accession phs000696.v1.p1.

Note: Any Supplementary Information and Source Data files are available in the online version of the paper.

ACKNOWLEDGMENTS

We thank M. Ducar for his assistance with genomic analyses; S. Chauvin for project management; L. Brown and H. Malkin for assisting with sample collection; T. Woo, B. Rich, R. Machaidze and D. Feldman for technical assistance; N. Stransky for the design of **Figure 2a**; and H. Taylor-Weiner and C.H. Brastianos for critical review of the manuscript. This work was supported by the Jared Branfman Sunflowers for Life Fund for Pediatric Brain and Spinal Cancer Research, the Pediatric Low-Grade Astrocytoma (PLGA) Program (S.S., W.C.H. and Charles D. Stiles), Pedals for Pediatrics and the Clark Family (P.E.M. and M.W.K.), the Stahl Family Charitable Foundation (P.E.M.), the Stop & Shop Pediatric Brain Tumor Program (P.E.M. and M.W.K.), the Pediatric Brain Tumor Clinical and Research Fund (P.E.M. and M.W.K.), the Children's Brain Tumor Foundation and the V Foundation (S.S.). S.S. is supported by grant K08 NS064168,

and P.K.B. is supported by grant K12 CA090354-11, the Brain Science Foundation, Susan G. Komen for the Cure, the Terri Brodeur Breast Cancer Foundation, the Conquer Cancer Foundation and the American Brain Tumor Association.

AUTHOR CONTRIBUTIONS

P.K.B., P.E.M., M.W.K., G.G. and S.S. designed the study. P.K.B., A.T.-W., C.S., G.G. and S.S. wrote the manuscript. A.T.-W., P.K.B., C.S., A.R.T. and G.G. performed computational analyses. P.V.H. supervised the sequencing. S.S. and D.N.L. reviewed the histopathology, and S.S., D.N.L. and M.P.H. coordinated and reviewed the immunohistochemistry. K.L.L. managed the tissue repository. R.T.J., L.A.B., A.S., N.S., L.S. and M.L.C. coordinated sample acquisition, processed samples and coordinated and performed exome and targeted sequencing. P.K.B., W.C.H., D.D.-S., D.N.L., A.C.R., M.W.K., G.G. and S.S. supervised the study. H.G.W.L., E.R.L., I.F.D., R.M.S., P.B.S., J.Y.K.L., J.N.P., N.D.A., H.T., M.M.-L., M.S., F.J.R., P.E.M., A.C.R., D.D.-S., D.N.L. and S.S. identified and provided materials for sequencing and validation, as well as clinical information. M.S.L. provided the code and the data to generate **Figure 1**. All authors discussed the results and implications and edited the manuscript.

COMPETING FINANCIAL INTERESTS

The authors declare no competing financial interests.

1. Louis, D.N., Ohgaki, H., Wiestler, O.D. & Cavenee, W.K. *WHO Classification of Tumours of the Central Nervous System* 238–240 (International Agency for Research on Cancer, 2007).
2. Crotty, T.B. *et al.* Papillary craniopharyngioma: a clinicopathological study of 48 cases. *J. Neurosurg.* **83**, 206–214 (1995).
3. Duff, J. *et al.* Long-term outcomes for surgically resected craniopharyngiomas. *Neurosurgery* **46**, 291–302, discussion 302–305 (2000).
4. Weiner, H.L. *et al.* Craniopharyngiomas: a clinicopathological analysis of factors predictive of recurrence and functional outcome. *Neurosurgery* **35**, 1001–1010, discussion 1010–1011 (1994).
5. Dolecek, T.A., Propp, J.M., Stroup, N.E. & Kruchko, C. CBTRUS statistical report: primary brain and central nervous system tumors diagnosed in the United States in 2005–2009. *Neuro-oncol.* **14** (suppl. 5), v1–v49 (2012).
6. Liubinas, S.V., Munshey, A.S. & Kaye, A.H. Management of recurrent craniopharyngioma. *J. Clin. Neurosci.* **18**, 451–457 (2011).
7. Manley, P.E. *et al.* Sleep dysfunction in long term survivors of craniopharyngioma. *J. Neurooncol.* **108**, 543–549 (2012).
8. Barkhoudarian, G. & Laws, E.R. Craniopharyngioma: history. *Pituitary* **16**, 1–8 (2013).
9. Cushing, H. Intracranial tumors: notes upon a series of two thousand cases with surgical mortality percentages pertaining thereto. *JAMA* **100**, 284 (1932).
10. Buslei, R. *et al.* Common mutations of β-catenin in adamantinomatous craniopharyngiomas but not in other tumours originating from the sellar region. *Acta Neuropathol.* **109**, 589–597 (2005).
11. Kato, K. *et al.* Possible linkage between specific histological structures and aberrant reactivation of the Wnt pathway in adamantinomatous craniopharyngioma. *J. Pathol.* **203**, 814–821 (2004).
12. Sekine, S. *et al.* Craniopharyngiomas of adamantinomatous type harbor β-catenin gene mutations. *Am. J. Pathol.* **161**, 1997–2001 (2002).
13. Cibulskis, K. *et al.* Sensitive detection of somatic point mutations in impure and heterogeneous cancer samples. *Nat. Biotechnol.* **31**, 213–219 (2013).
14. Lawrence, M.S. *et al.* Mutational heterogeneity in cancer and the search for new cancer-associated genes. *Nature* **499**, 214–218 (2013).
15. Brastianos, P.K. *et al.* Genomic sequencing of meningiomas identifies oncogenic *SMO* and *AKT1* mutations. *Nat. Genet.* **45**, 285–289 (2013).
16. Futreal, P.A. *et al.* A census of human cancer genes. *Nat. Rev. Cancer* **4**, 177–183 (2004).
17. Stanley, F.K., Moore, S. & Goodarzi, A.A. CHD chromatin remodelling enzymes and the DNA damage response. *Mutat. Res.* **750**, 31–44 (2013).
18. Laczmanska, I. & Sasiadek, M.M. Tyrosine phosphatases as a superfamily of tumor suppressors in colorectal cancer. *Acta Biochim. Pol.* **58**, 467–470 (2011).
19. Jones, D.T. *et al.* Oncogenic *RAF1* rearrangement and a novel *BRAF* mutation as alternatives to *KIAA1549:BRAF* fusion in activating the MAPK pathway in pilocytic astrocytoma. *Oncogene* **28**, 2119–2123 (2009).
20. Tian, Y. *et al.* Detection of *KIAA1549-BRAF* fusion transcripts in formalin-fixed paraffin-embedded pediatric low-grade gliomas. *J. Mol. Diagn.* **13**, 669–677 (2011).
21. Capper, D. *et al.* Assessment of BRAF V600E mutation status by immunohistochemistry with a mutation-specific monoclonal antibody. *Acta Neuropathol.* **122**, 11–19 (2011).
22. Anastas, J.N. & Moon, R.T. WNT signalling pathways as therapeutic targets in cancer. *Nat. Rev. Cancer* **13**, 11–26 (2013).
23. Basu, A. *et al.* An interactive resource to identify cancer genetic and lineage dependencies targeted by small molecules. *Cell* **154**, 1151–1161 (2013).
24. Chapman, P.B. *et al.* Improved survival with vemurafenib in melanoma with BRAF V600E mutation. *N. Engl. J. Med.* **364**, 2507–2516 (2011).
25. Flaherty, K.T. *et al.* Inhibition of mutated, activated BRAF in metastatic melanoma. *N. Engl. J. Med.* **363**, 809–819 (2010).
26. Ribas, A. & Flaherty, K.T. BRAF targeted therapy changes the treatment paradigm in melanoma. *Nat. Rev. Clin. Oncol.* **8**, 426–433 (2011).
27. Sosman, J.A. *et al.* Survival in BRAF V600–mutant advanced melanoma treated with vemurafenib. *N. Engl. J. Med.* **366**, 707–714 (2012).
28. Chamberlain, M.C. Salvage therapy with BRAF inhibitors for recurrent pleomorphic xanthoastrocytoma: a retrospective case series. *J. Neurooncol.* **114**, 237–240 (2013).
29. Rush, S., Foreman, N. & Liu, A. Brainstem ganglioglioma successfully treated with vemurafenib. *J. Clin. Oncol.* **31**, e159–e160 (2013).
30. Ascierto, P.A. *et al.* Phase II trial (BREAK-2) of the BRAF inhibitor dabrafenib (GSK2118436) in patients with metastatic melanoma. *J. Clin. Oncol.* **31**, 3205–3211 (2013).
31. Sievert, A.J. *et al.* Paradoxical activation and RAF inhibitor resistance of BRAF protein kinase fusions characterizing pediatric astrocytomas. *Proc. Natl. Acad. Sci. USA* **110**, 5957–5962 (2013).
32. Dietrich, S. *et al.* BRAF inhibition in refractory hairy-cell leukemia. *N. Engl. J. Med.* **366**, 2038–2040 (2012).
33. Dias-Santagata, D. *et al.* BRAF V600E mutations are common in pleomorphic xanthoastrocytoma: diagnostic and therapeutic implications. *PLoS ONE* **6**, e17948 (2011).
34. Schindler, G. *et al.* Analysis of BRAF V600E mutation in 1,320 nervous system tumors reveals high mutation frequencies in pleomorphic xanthoastrocytoma, ganglioglioma and extra-cerebellar pilocytic astrocytoma. *Acta Neuropathol.* **121**, 397–405 (2011).
35. MacConaill, L.E. *et al.* Profiling critical cancer gene mutations in clinical tumor samples. *PLoS ONE* **4**, e7887 (2009).

ONLINE METHODS

Sample selection and preparation. The study was reviewed and approved by the human subjects institutional review boards of the Dana-Farber Cancer Institute, Brigham and Women's Hospital, Broad Institute of Harvard and MIT, Boston Children's Hospital, Johns Hopkins Hospital, Children's Cancer Hospital Egypt and Children's Hospital of Philadelphia. Written informed consent was obtained from all participants whose tumor samples were subjected to whole-exome sequencing. Histologic diagnosis was reconfirmed on all samples by a board-certified neuropathologist (S.S.), and representative fresh-frozen and paraffin-embedded blocks with estimated purity ≥10% were selected. DNA was extracted from tissue shavings of frozen tissue or 1-mm core-punch biopsies (Miltex, 33-31AA-P/25) from formalin-fixed paraffin-embedded tissue and from buffy coat preparations of paired blood using standard techniques (QIAGEN, Valencia, CA). The DNA was then quantified using PicoGreen dye (InVitrogen, Carlsbad CA). Mass spectrometric genotyping with a well-established 48-SNP panel was used to confirm the identity of tumor-normal pairs (Sequenom, San Diego, CA)[36].

Whole-exome sequencing and analyses. Whole-exome sequencing was performed as previously described[15]. In brief, DNA was fragmented by sonication (Covaris Inc., Woburn, MA) to 150 bp and further purified using Agencourt AMPure XP beads. 50 ng of size-selected DNA was then ligated to specific adaptors during library preparation (Illumina TruSeq, Illumina Inc., San Diego, CA). Each library was made with sample-specific barcodes and quantified by quantitative PCR (Kapa Biosystems, Inc., Woburn, MA), and two libraries were pooled to a total of 500 ng for exome enrichment using the Agilent SureSelect hybrid capture kit (Whole Exome_v2 and Whole Exome_v4, 44 Mb; Agilent Technologies, Santa Clara, CA). Several captures were pooled further and sequenced in one or more lanes to a final equivalent of two exomes per lane on a HiSeq 2500 system (Illumina Inc, San Diego, CA).

Read pairs were aligned to the hg19 reference sequence using the Burrows-Wheeler Aligner[37], and sample reads were demultiplexed using Picard tools. Data were sorted and duplicate-marked using SAMtools and Picard. Bias in base quality score assignments due to flowcell, lane, dinucleotide context and machine cycle were analyzed and recalibrated, and local realignment around insertions or deletions (indels) was achieved using the Genome Analysis Toolkit (GATK)[38,39]. Somatic variant calling was performed within the Firehose environment[40] using MuTect[13]. All sample pairs passed a quality-control pipeline to test for any tumor-normal and interindividual mixups by comparing insert-size distribution and copy-number profile as described previously[41].

Somatic mutations and short indels were called and post filtered using MuTect[13] and IndelLocator[40,41]. These were annotated to genes and compared to events in the Catalogue of Somatic Mutations in Cancer (COSMIC) using Oncotator, and spurious calls caused by mismapping and other previously identified systematic errors were removed using an established list of known problematic sites[15,40,42,43]. MutSig[14] was used to determine the significance of mutated genes. MutSig compares observed mutations against expected sequence-specific, context-specific, tumor-specific and gene-specific background mutation frequencies. Additionally MutSig prioritizes mutations that are positionally clustered or occur in highly conserved regions[40,42,43]. We analyzed mutational spectra and rates across multiple tumor types using previously described methods[14].

Mutation clonality analysis. To assess whether mutations are clonal (i.e., present in all cancer cells), we assessed the CCF of each mutation, as described in Carter *et al.*[44]. Mutations for which the CCF is close to 1 are considered clonal. Those mutations with lower probable CCFs are considered subclonal. To determine the CCF, we first calculated the sample purity (i.e., the percentage of tumor cells in our sample) by constructing the probability density function for the allele fractions of mutations. Using that information, we then identified a clonal heterozygous peak at or below 0.5 allele fraction:

$$\mathrm{pdf}(\mathrm{af}) = \sum_m \beta_{\mathrm{pdf}}(\mathrm{af}, \mathrm{alt}(m)+1, \mathrm{ref}(m)+1)$$

where af is the true allele fraction between 0 and 1, alt is the alternate allele counts, ref is the reference allele counts and m is the index for mutation count[44]. We assumed that the local copy number at each mutation is 2 for craniopharyngioma and that each tumor has heterozygous clonal mutations that are sufficient to form a peak[45,46]. Given these assumptions, the purity is the peak af × 2.

Once we estimated tumor purity, we then estimated the CCF for each mutation. The CCF is the percentage of tumor cells harboring a given mutation. Clonal mutations have a true CCF of 1, and subclonal mutations have a true CCF <1. The observed allele counts correspond to a probability density of the CCF, which can be estimated with the following equation:[44]

$$\mathrm{pdf}(\mathrm{CCF}, m) = \beta_{\mathrm{pdf}}\left(\frac{\mathrm{CCF}}{\mathrm{CN}(m)} \times \mathrm{purity}, \mathrm{alt}(m)+1, \mathrm{ref}(m)+1\right)$$

where CN(m) is the local copy number at the given mutation m, and CCF ranges from 0 to 1. The probability for any allele fraction greater than the maximum CCF allowed was folded back to a CCF of 1. We again assumed a copy number of 2 (refs. 26,27). We also considered the possibility that the site is homozygous in both copies of the chromosome (loss of heterozygosity) by multiplying the CCF by 2 in the equation above and chose the solution with the highest peak probability. The CCF formulation is approximately equivalent to ABSOLUTE[44]. The pdfs also provided a direct estimate of the confidence intervals on CCF. Each mutation was classified as clonal or subclonal on the basis of the probability that the CCF exceeded 0.80. A probability threshold of 0.5 was used throughout for this classification[47].

Validation of candidate mutations by Sequenom genotyping and SNaPshot. We validated all of the common mutations in *BRAF* and *CTNNB1* by mass spectrometric genotyping based on the Sequenom MassARRAY technology (Sequenom Inc, San Diego, CA) using a multibase homogenous Mass-Extend (hME) as previously described[35,48]. The complete hME assay list is provided in **Supplementary Table** 3. A second targeted sequencing platform (SNaPshot genotyping) was performed as previously described to validate the BRAF p.Val600Glu (c.1799T>A) alteration in all papillary craniopharyngiomas[33,49,50].

IHC. We performed immunohistochemical studies on 5-µm-thick whole-tissue sections of formalin-fixed paraffin-embedded tissue in a Bond 3 automated immunostainer (Leica Microsystems, Bannockburn, IL, USA) using a primary antibody against BRAF p.Val600Glu (clone VE1, 1:100, Spring Bioscience, Pleasanton, CA) and a primary antibody against β-catenin (see below). For BRAF p.Val600Glu, we deparaffinized the sections on the Leica Bond using Bond Dewax solution and performed antigen retrieval with an ethylenediaminetetraacetic acid–based solution (Leica) at pH 9 and a Leica Polymer Refine kit for DAB (diaminobenzidine) staining. Appropriate positive and negative controls were included. Positive staining was characterized by diffuse and moderate cytoplasmic staining of the tumor cells. We considered isolated nuclear staining, weak staining of occasional cells or faint diffuse staining as negative staining. For β-catenin (BD Pharmingen, 610154, mouse monoclonal, clone 14), antigen retrieval was performed in a pressure cooker in citrate buffer (pH 6.0, 1:1,000 dilution) with a 45-min incubation followed by Dako anti-mouse horseradish peroxidase for 30 min at room temperature. Cases with nuclear staining (which ranged from low level to high level) were scored as positive, and cases with membranous staining were scored as negative.

36. Demichelis, F. *et al.* SNP panel identification assay (SPIA): a genetic-based assay for the identification of cell lines. *Nucleic Acids Res.* **36**, 2446–2456 (2008).
37. Li, H. & Durbin, R. Fast and accurate short read alignment with Burrows-Wheeler transform. *Bioinformatics* **25**, 1754–1760 (2009).
38. DePristo, M.A. *et al.* A framework for variation discovery and genotyping using next-generation DNA sequencing data. *Nat. Genet.* **43**, 491–498 (2011).
39. McKenna, A. *et al.* The Genome Analysis Toolkit: a MapReduce framework for analyzing next-generation DNA sequencing data. *Genome Res.* **20**, 1297–1303 (2010).
40. Chapman, M.A. *et al.* Initial genome sequencing and analysis of multiple myeloma. *Nature* **471**, 467–472 (2011).

doi:10.1038/ng.2868

41. Berger, M.F. *et al.* The genomic complexity of primary human prostate cancer. *Nature* **470**, 214–220 (2011).
42. Lohr, J.G. *et al.* Discovery and prioritization of somatic mutations in diffuse large B-cell lymphoma (DLBCL) by whole-exome sequencing. *Proc. Natl. Acad. Sci. USA* **109**, 3879–3884 (2012).
43. Stransky, N. *et al.* The mutational landscape of head and neck squamous cell carcinoma. *Science* **333**, 1157–1160 (2011).
44. Carter, S.L. *et al.* Absolute quantification of somatic DNA alterations in human cancer. *Nat. Biotechnol.* **30**, 413–421 (2012).
45. Rickert, C.H. & Paulus, W. Lack of chromosomal imbalances in adamantinomatous and papillary craniopharyngiomas. *J. Neurol. Neurosurg. Psychiatry* **74**, 260–261 (2003).
46. Yoshimoto, M. *et al.* Comparative genomic hybridization analysis of pediatric adamantinomatous craniopharyngiomas and a review of the literature. *J. Neurosurg.* **101**, 85–90 (2004).
47. Landau, D.A. *et al.* Evolution and impact of subclonal mutations in chronic lymphocytic leukemia. *Cell* **152**, 714–726 (2013).
48. Thomas, R.K. *et al.* High-throughput oncogene mutation profiling in human cancer. *Nat. Genet.* **39**, 347–351 (2007).
49. Corcoran, R.B. *et al. BRAF* gene amplification can promote acquired resistance to MEK inhibitors in cancer cells harboring the BRAF V600E mutation. *Sci. Signal.* **3**, ra84 (2010).
50. Dias-Santagata, D. *et al.* Rapid targeted mutational analysis of human tumours: a clinical platform to guide personalized cancer medicine. *EMBO Mol. Med.* **2**, 146–158 (2010).